INTERFACE

royalsocietypublishing.org/journal/rsif

Research

**Cite this article:** Suen JY, Navlakha S. 2019 Travel in city road networks follows similar transport trade-off principles to neural and plant arbors. *J. R. Soc. Interface* **16**: 20190041. http://dx.doi.org/10.1098/rsif.2019.0041

Received: 21 January 2019
Accepted: 15 April 2019

**Subject Category:**
Life Sciences–Engineering interface

**Subject Areas:**
computational biology, biomathematics, bioinformatics

**Keywords:**
network theory, Pareto optimality, transport networks, biological networks

**Author for correspondence:**
Jonathan Y. Suen
e-mail: jsuen@ece.ucsb.edu

Electronic supplementary material is available online at https://dx.doi.org/10.6084/m9.figshare.c.4483382.

THE ROYAL SOCIETY PUBLISHING

# Travel in city road networks follows similar transport trade-off principles to neural and plant arbors

Jonathan Y. Suen and Saket Navlakha

The Salk Institute for Biological Studies, Integrative Biology Laboratory, La Jolla, CA 92037, USA

JYS, 0000-0002-9803-5900; SN, 0000-0002-5505-9718

Both engineered and biological transportation networks face trade-offs in their design. Network users desire to quickly get from one location in the network to another, whereas network planners need to minimize costs in building infrastructure. Here, we use the theory of Pareto optimality to study this design trade-off in the road networks of 101 cities, with wide-ranging population sizes, land areas and geographies. Using a simple one parameter trade-off function, we find that most cities lie near the Pareto front and are significantly closer to the front than expected by alternate design structures. To account for other optimization dimensions or constraints that may be important (e.g. traffic congestion, geography), we performed a higher-order Pareto optimality analysis and found that most cities analysed lie within a region of design space bounded by only four archetypal cities. The trade-offs studied here are also faced and well-optimized by two biological transport networks—neural arbors in the brain and branching architectures of plant shoots—suggesting similar design principles across some biological and engineered transport systems.

## 1. Introduction

Networks face trade-offs between conflicting goals. In engineering, this trade-off is often between the performance of the network, benefiting individual users, and the costs of constructing the network. Users desire to transport a payload, such as information or a physical object, at an unlimited capacity and at the fastest speed possible. Conversely, a network fulfilling these goals is expensive to construct, consuming significant resources, such as money, space and energy. Thus, network designers seek to build networks that are efficient, maximizing benefits provided by allocated resources.

Nearly all engineered networks are subject to this trade-off. For example, a data network, like the Internet, would need dedicated links between every pair of users to achieve maximum performance, since high bandwidth and low latency are desired by the user. To the network provider, however, the number and length of physical links impose major costs [1,2]. Similar trade-offs are also faced by water pipeline networks [3], power grids [4] and wireless sensor networks [5]. In practice, most networks are not likely to be optimally efficient due to constraints (e.g. mountains that necessitate a circuitous path) or difficulty in modifying or pruning certain parts of the network in response to changing user demands. There may also be other factors to optimize in the network, such as reliability and robustness [2].

Here, we study travel paths in metropolitan area road networks, where users in suburban locations desire to commute downtown. We make the following contributions:

(1) We collected travel paths for 11 615 users over 101 cities worldwide, with metro area populations ranging from 7000 to 38 million, with city proper land areas ranging from 5 to 16 400 $km^2$, and with a variety of geographical constraints, including rivers and bays, mountainous terrain and geopolitical boundaries (figure 1*a*).

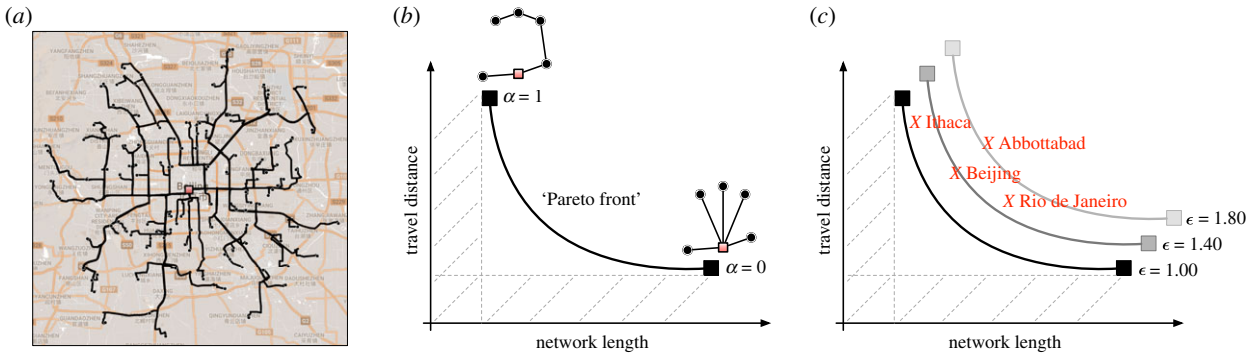


**Figure 1.** Pareto optimality analysis of travel paths. (*a*) Travel paths from randomly distributed points in Beijing to a central downtown location (Tiananmen Square), as provided by Google Maps. (*b*) The Pareto front that optimally trades-off construction costs ($\alpha = 1$) and travel distance ($\alpha = 0$). The variable $\alpha$ defines the relative weights between the two competing goals. (*c*) Example cities that lie close (Ithaca) and far (Abbottabad) to the Pareto front. The distance to the Pareto front is calculated using a variable $\epsilon$. Cities with $\epsilon > 1$ require greater construction costs and/or travel distance than a Pareto-optimal city. This diagram is only to illustrate how $\epsilon$ can vary across cities; in reality, different road networks likely have different Pareto fronts. (Online version in colour.)

(2) We study the trade-off between travel distance (user performance) and total network length (road cost). We use a network design algorithm to generate near-Pareto optimal topologies that balance between these two competing objectives based on a single parameter ($\alpha$) denoting how the two objectives are weighted against each other. We find that many, though not all, cities lie near the Pareto front with a surprisingly tight range of $\alpha$ values. This indicates similar balancing of the two objectives across cities, despite the broad diversity in population, city size and region.
(3) We find that when three additional time-related optimization measures (speed, congestion and number of manoeuvres) are added to travel distance and network length, the dimensionality of the data increases by only one, i.e. most cities lie within a three-dimensional subspace. The polytope that bounds all cities within this subspace has four corners, representing four archetypical cities: Jerusalem, Juba, Amarillo and Delhi. These cities formed extremum in trade-offs, some favouring optimizing network length (Jerusalem and Juba), optimizing travel distance (Amarillo and Delhi) and optimizing travel speed (Amarillo), while also performing poorly in handling congestion (Delhi) and minimizing travel distances (Jerusalem). Our results suggest a certain simplicity to the structure of global travel paths that have emerged through various growth processes.

We conclude by discussing analogous trade-offs faced in biological networks, and how the study of one may shed light on the other.

## 2. Related work

Prior work has largely focused on analysing the structure of road networks as graphs, or on developing highly parameterized models of traffic flow and routing. Our focus instead is on quantifying the trade-off between user performance and network length in road structures using travel path data from numerous cities.

### 2.1. Analysing road structures as graphs

Graphs are a common abstraction used to analyse the structure of road networks [6,7]. Such analyses have shown, for example, that roads form scale-free networks [8] and display self-similarity [9]. Others have studied the hierarchy of road networks, ranging from slow residential streets with many intersections to large controlled-access highways. These works studied the structural properties (e.g. 'beltness', 'treeness', etc.) used in each layer of the hierarchy, and the interfaces between layers [7]. Prior works have also studied how to optimally redesign existing road structures by integrating data on connectivity, broad geography and road usage statistics [10]. However, there are many external factors that affect the design and routing of roads, especially on a sub-kilometre scale. This includes local terrain (small hills, ravines and subsurface geology) [11], environmental concerns (noise, pollution), land acquisition costs, and political factors [12], among others. While broad scale geography, at 1 km resolution, has been analysed to determine where roads should be built [13], it is difficult to gather the data necessary to generate a representative model on a city level.

In contrast to these works, we derive a measure to describe the network not in a strictly topological or structural sense, but rather in terms of a user-network trade-off. The focus of this trade-off is on travel paths, which describe how the underlying roads are used to get from one location in the network to another, while implicitly taking road type into account. In contrast to previous studies that only study one road type, or that treat all road types as identical [7–9,14,15], our travel paths consider residential streets, central arteries and freeways together; we are also able to study more rural and lesser-developed cities, which may not have larger types of roads. Previous studies using travel paths have focused on morphological features, such as 'inness' [16], but have not studied the user-network trade-off. The user optimality of small-scale non-road networks has been explored before [17], but has not been applied to the continuum of network topologies between user optimal and network optimal configurations.

### 2.2. Models of traffic flow and routing

There are many features important to road travel that are not captured by static analysis of road graphs. To get from one location in the network to another, a user will often travel on different types of roads, such as surface streets, arteries and highways. Determining realistic travel paths given a map is thus often done by either applying a routing

algorithm [18], or by collecting empirical data [19]. The decision process for a user to select between these types of roads has been modelled in terms of a continuous flow on a discrete network [20], or as an empirical factor based on probabilistic processes [18]. Accurate routing algorithms must also be privy to other roadway characteristics such as intersection types (e.g. a two-way versus a four-way stop) and utilization (e.g. unprotected turns against traffic), and the effects of varying capacity, speed limits and traffic congestion. However, these factors can vary significantly based on local environmental factors and may not be apparent from large-scale mapping data [21].

Routing algorithms are further complicated in that a user would like to reach the destination in both the fastest time and shortest travel distance possible. When this is not possible, users are willing to trade-off some additional distance travelled for a reduction in travel time, as exhibited by drivers travelling a longer route to avoid traffic congestion and delay at intersections [22]. In routing algorithms, this trade-off is described by a variable equal to the assumed cost per minute of travel time divided by the assumed cost per kilometre travelled (sometimes called the cost index [23]). Other studies have analysed how travel times can be decreased if vehicles were routed using centrally determined, system-optimal paths rather than user-optimal paths [24], whereas our more realistic scenarios assume ordinary greedy driver behaviour.

Rather than developing a complex traffic model and routing algorithm for each city, or limiting our study to certain model structures [20], we used the routing algorithms developed by Google Maps [25]. Though we treat Google Maps as a 'black box', the travel paths suggested by Google Maps are followed by millions of users every day and are generally regarded as accurate. Notably, Google Maps has a traffic congestion and travel time model based on crowdsourced empirical data. The unmatched scale and quality of Google Maps allows us to sample long routes over hundreds of square kilometres, across 101 global cities, in a uniform manner and more accurately than theoretical models.

### 2.3. Relationship to biological network design and routing

Our study is also motivated by similar network design trade-offs that occur in biology. For example, Conn *et al.* [26] showed that plant architectures can also be viewed as transport networks, used to shuttle nutrients from one organ of the plant to another. These networks also must straddle between optimizing for fast nutrient transport (user performance) while also balancing for costs in building the architecture (network cost). Similarly, Budd *et al.* [27] and Cuntz *et al.* [28] showed that neural arbors (dendrites and axons) can also be viewed as transport networks used to shuttle information (action potentials or signals) from one neuron to another. These networks must balance between the distance or time required to route the signal along the arbor (user performance) versus the amount of wiring needed to realize a specific topology given a space-constrained brain (network cost). Prior work has suggested that both of these systems have evolved mechanisms to generate Pareto-optimal topologies [29]. Our goal here is to test these ideas in human engineered road networks that have likely evolved using different mechanisms.

### 2.4. Additional work in Pareto optimality of complex networks

Seoane and Sole [30,31] study a trade-off between network efficiency and cost using Pareto optimization, and they study how these competing forces can lead to phase transitions in design space, also called network morphospace [32]. Our work studies a specific example of this morphospace as instantiated by travel paths in cities. Moses *et al.* [33] study trade-offs between minimizing delivery time and energy dissipation required for delivery of a resource, and they find scaling principles between the two in vascular networks and computer chip designs. Thus, while the idea of studying network design trade-offs across engineered and biological contexts is not new, our study instantiates these ideas in a specific domain of single-source transport systems.

## 3. Results

First, we describe a framework based on the theory of Pareto optimality to study user-performance trade-offs in road network travel paths. Second, we analyse travel paths in 101 cities and show that most fall significantly closer to the Pareto front than expected with surprisingly little variability in how different cities trade-off competing objectives. Third, we analyse the travel paths using a higher-order Pareto optimization and show that all cities can be bounded within a small region of trait space, exemplified by four archetype cities.

### 3.1. A framework for quantifying user-network trade-offs in road structures

The idea of the Pareto front is often used in engineering and economics to find optimal trade-offs between competing objectives [34–36]. This theory has had a long history of being used to study trade-offs in biological systems [37–40], for which evolution and natural selection are hypothesized to optimize biological function with respect to competing demands. Intuitively, consider two competing objectives, $o_1$ and $o_2$. If some solution $a_1$ outperforms solution $a_2$ on both objectives, then $a_1$ is said to 'dominate' $a_2$, leading to $a_2$ being removed from the population. Repeating this argument for all possible solutions, the only solutions that remain lie along the Pareto front of $o_1$ and $o_2$. This front is defined as the set of solutions where increasing the performance on one objective necessarily results in a loss in performance on the other objective (figure 1*b*)

In our case, we are given as input a set of points, $\mathcal{P} = \{p_1, p_2, \ldots, p_n\}$, corresponding to the 2D locations of $n$ random users in a city; and a root point $r$, corresponding to the location of downtown, where the users seek to travel to (Methods). Our goal is to output a tree $G = (V, E)$, where $V = \mathcal{P} \cup \{r\}$, and $E$ are the set of edges connecting the nodes in $V$.

The first objective is to minimize the road cost (network length), which is equal to the sum of all the edge lengths:

$$C(G) = \sum_{(u,v)\in E} \mathrm{d}(u, v), \tag{3.1}$$

where $\mathrm{d}(u, v)$ is the Euclidean distance between $u$ and $v$. Ideally, all points in $\mathcal{P}$ would have the same position relative to downtown for all cities. This was not possible because some

points for a given city may lie in bodies of water or uninhabited areas (Methods). We thus normalized $C(G)$ by the mean straight-line distance between $r$ and each $p_i \in \mathcal{P}$.

The second objective is to minimize the user travel distances, which is equal to the sum of the distances from each point to the root (downtown):

$$T(G) = \sum_i l(G, p_i, r), \tag{3.2}$$

where $l(G, p_i, r)$ is the distance to travel from $p_i$ to $r$ along the edges in $G$. Similar to the reasoning above, $T(G)$ was normalized by the sum of straight-line distances.

Both of these measures are clearly approximations of actual performance and cost. For example, network length is one aspect of road costs, but there are other factors, as well, including the number of lanes and the terrain. Travel distance itself can be determined fairly accurately; however, users also assign value to minimizing travel time. Distance and time are often correlated—the shortest path is often the fastest path—but there are factors such as roadway speeds, traffic congestion and intersection delays. We consider these and other factors in our higher-order Pareto analysis discussed later.

The objectives of minimizing network length and minimizing travel distance are at odds with one another. For example, minimizing network length is achieved by a minimum spanning tree of the graph (or a Steiner tree, if branch points are allowed). This solution, however, would not be very attractive from a user's perspective, who may have to travel long distances to get to downtown. On the other hand, minimizing travel distance is achieved using a 'satellite' tree, where the root is connected via a straight line to each user location. However, this solution would not be very attractive from a network cost perspective since it would require significant resources to build. These two cases bound possible networks: there can be no shorter travel distance than the straight-line paths of the satellite tree, nor can network costs be lower than the Steiner tree.

One natural way to define an optimization function that incorporates these two objectives together is to solve:

$$\begin{aligned} &\text{minimize} \quad T(G) \\ &\text{subject to} \\ &\quad C(G) < B, \end{aligned} \tag{3.3}$$

where $B$ is a budget on the total length of the network. This formulation sets the network length to be a hard constraint. To soften this constraint, we seek to solve:

$$\text{minimize} \quad \alpha C(G) + (1 - \alpha)T(G), \tag{3.4}$$

where $0 \leq \alpha \leq 1$ is a parameter (similar to the Lagrange multiplier) that controls how much weight or priority should be placed on each objective. For example, if $\alpha \approx 0$, then the network promotes minimizing travel distance and would look satellite-like. If $\alpha \approx 1$, then the network promotes minimizing total length and would look closer to a spanning tree. Importantly, this parameter $\alpha$ provides a single number representing how a network trades-off these two objectives.

The Pareto front consists of solutions to equation (3.4) for all values of $\alpha \in [0, 1]$. This front is also bounded by the two extremal networks, the satellite and a minimum spanning tree. The objective in equation (3.4) is clearly NP-hard, as it equals the Steiner tree problem for $\alpha = 1$. We, therefore, use an empirically near-optimal greedy algorithm [26] to compute the Pareto front (Methods). Each city has its own Pareto front defined by $r$ and $\mathcal{P}$ (its set of $n$ user locations). The use of a single downtown destination allowed us to examine travel paths towards a primary location in a city. Large cities may have multiple population centres, and our framework can similarly be used to analyse these polycentric structures.

## 3.2. Comparison to baseline networks

To establish a baseline to compare how close a city lies to the Pareto front, we compared with two baseline architectures. The first baseline, Random, creates a random spanning tree using the points $\mathcal{P}$ and $r$ as input and is used to test whether Pareto optimality can be achieved trivially. The second baseline, PrefAttach, uses the Barabasi–Albert model [41] to build a tree on the input points. This generative graph model starts with two random nodes connected by an edge. Then, in each iteration of the algorithm, it connects a new node to one existing node biased by the degree of the existing node. This results in a 'rich get richer' scale-free tree, with many potential hubs, as are commonly found in many transport networks.

## 3.3. Quantifying optimality, i.e. the distance to the Pareto front

For each city, we computed both its value of $\epsilon$ (how far away it is to the Pareto front) and $\alpha$ (where it lies on the scaled Pareto front).

Given the network $G$ of a city, we can compute its values for $x = C(G)$ and $y = T(G)$. Call this point $p_G = (x, y)$. To determine how far away $p_G$ lies from the Pareto front, we scaled the Pareto front until it intersected with $p_G$, and we then used the amount of scaling required as a measure of optimality. Specifically, let the Pareto front be defined by a set of points, $\{(x_1, y_1), (x_2, y_2), \ldots, (x_k, y_k)\}$, where $(x_i, y_i)$ corresponds to the optimal travel distance and total length of the network for $\alpha_i$. To scale the front, we multiply each $(x_i, y_i)$ pair by a small value $\epsilon > 1$ and test if this new Pareto front intersects with $p_G$. We keep increasing the value of $\epsilon$ until it intersects with $p_G$. The larger the value of $\epsilon$, the further away the network lies to the Pareto front (figure 1*c*). If the network lies exactly on the Pareto front, its $\epsilon = 1.0$.

This scaling allows a direct interpretation of $\epsilon$: a city with $\epsilon = 1.5$ imposes the same road length and travel distance as a Pareto-optimal city with the points $\mathcal{P}$ with radius 1.5 times farther from the root. This is more explanatory than computing the Euclidean distance (in kilometres) from $p_G$ to the closest point on the Pareto curve, since this distance combines two indirectly related lengths (network length and travel distance). Our method determines the Pareto trade-off $\alpha$ that results in the smallest $\epsilon$, in contrast to other methods, such as the one utilized by Gastner *et al.* [17] which strictly assumes $\alpha = 0$.

## 3.4. Using Google Maps to infer travel paths in a city

We used Google Maps to collect travel paths for 11 615 users in 101 global cities. These cities spanned different geographical regions, sizes, ages and levels of economic development. For example, cities had metropolitan area populations ranging from 7000 (Great Barrington, MA, USA) to 38 million (Tokyo, Japan), and had city land areas ranging from 5 km (Byblos,

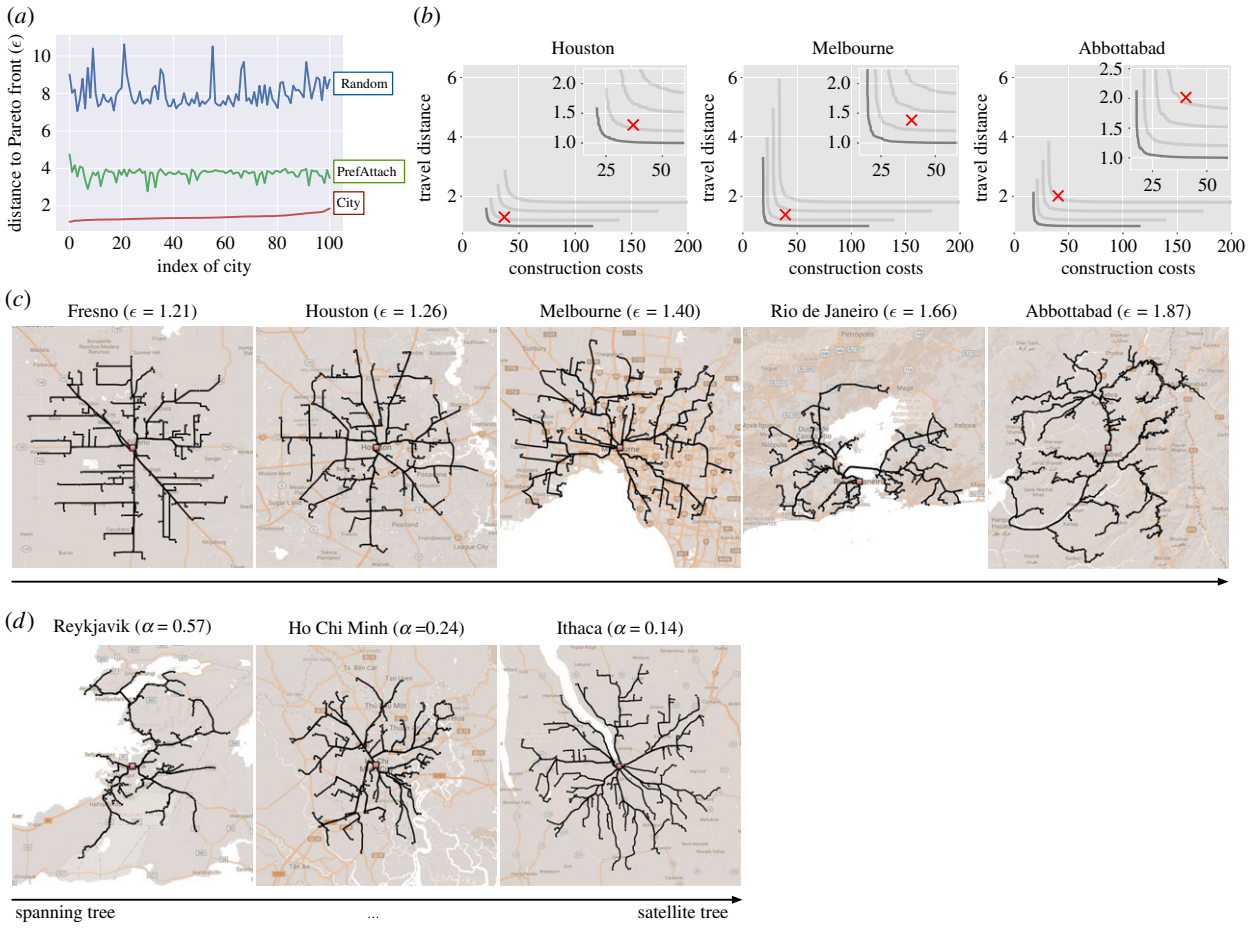


**Figure 2.** Pareto efficiency. (*a*) Distance to the Pareto front, denoted by $\epsilon$ (*y*-axis), of travel paths from all cities was significantly lower than two random network models. (*b*) Example Pareto fronts for a city close to the Pareto front (Houston), far from the Pareto front (Abbottabad) and in between (Melbourne). The dark curve shows the Pareto front with $\epsilon = 1$. The light curves show scaled Pareto fronts with $\epsilon = 1.2$, 1.5 and 1.8. The 'X' denotes where the city lies. (*c*) Travel paths in cities spanning the range of $\epsilon$ observed (map data: Google, INEGI). (*d*) Cities with varying $\alpha$, ranging from Reykjavik, the most spanning tree-like city analysed, to Ithaca, the third-most satellite-tree city. (map data: Google). (Online version in colour.)

Lebanon) to 16 400 km (Beijing, China). The oldest city (Byblos, Lebanon) has been inhabited for 7000 years, and we also included newly built cities, such as Brasilia, Brazil and Abuja, Nigeria, (founded 1960 and 1984, respectively). The diversity of city features considered here makes this dataset a strong benchmark for studying any principle of travel paths.

For each city, we selected $n = 115$ random locations ($P$), which each had a uniformly distributed random 360° azimuth and radius $\rho \in [5, 30]$ km from a centrally located point (downtown) $r$. The point $r$ was in the central business district of the city, most often a city hall or central monument. We then obtained the travel paths from each $p_i \in \mathcal{P}$ to $r$ for every city. To compute the network length $C(G)$, we formed a tree $G$ by merging all paths and deleting overlapping segments, then summing the lengths of all the edges. To compute the travel distance $T(G)$, we summed the lengths of all 115 travel paths (Methods).

## 3.5. Other objectives of interest

Google Maps' suggested travel paths incorporate factors that we do not explicitly try to optimize with our greedy algorithm, including time spent waiting at intersections, speed limits, and traffic congestion. As discussed previously, as opposed to developing detailed and highly parameterized routing and road construction models, our goal is to use network length and travel distance as a proxy for construction costs and travel times, to determine how much these two simple factors alone dictate the structure of travel paths. Later, we also use a higher-order Pareto optimality technique to incorporate a number of these other factors, including traffic congestion and travel time.

## 3.6. Are travel paths in city road networks close to being Pareto optimal?

For each city, we used as input the locations of the $n$ random points $\mathcal{P}$ in the city, and the location of downtown ($r$). We used the greedy algorithm to generate a set of Pareto-optimal trees for this city by varying $\alpha \in [0, 1]$. We then computed the network length and travel distance for the actual city's road network and assessed how far the city was from the Pareto front ($\epsilon$). Using the same set of points, we also computed the distance to the Pareto front for two baseline networks (Random and PrefAttach, averaged over 1000 trees) to assess significance.

We found that the travel paths in every city were closer to the Pareto front than the baseline networks (figure 2*a*). For example, the distance to the Pareto front for Beijing was $\epsilon = 1.36$, compared to 3.82 and 7.47 for PrefAttach and Random, respectively. This indicates that achieving the level of Pareto optimality achieved by the city road network is not trivial. This also suggests that despite the diverse constraints faced by actual road topologies compared to our

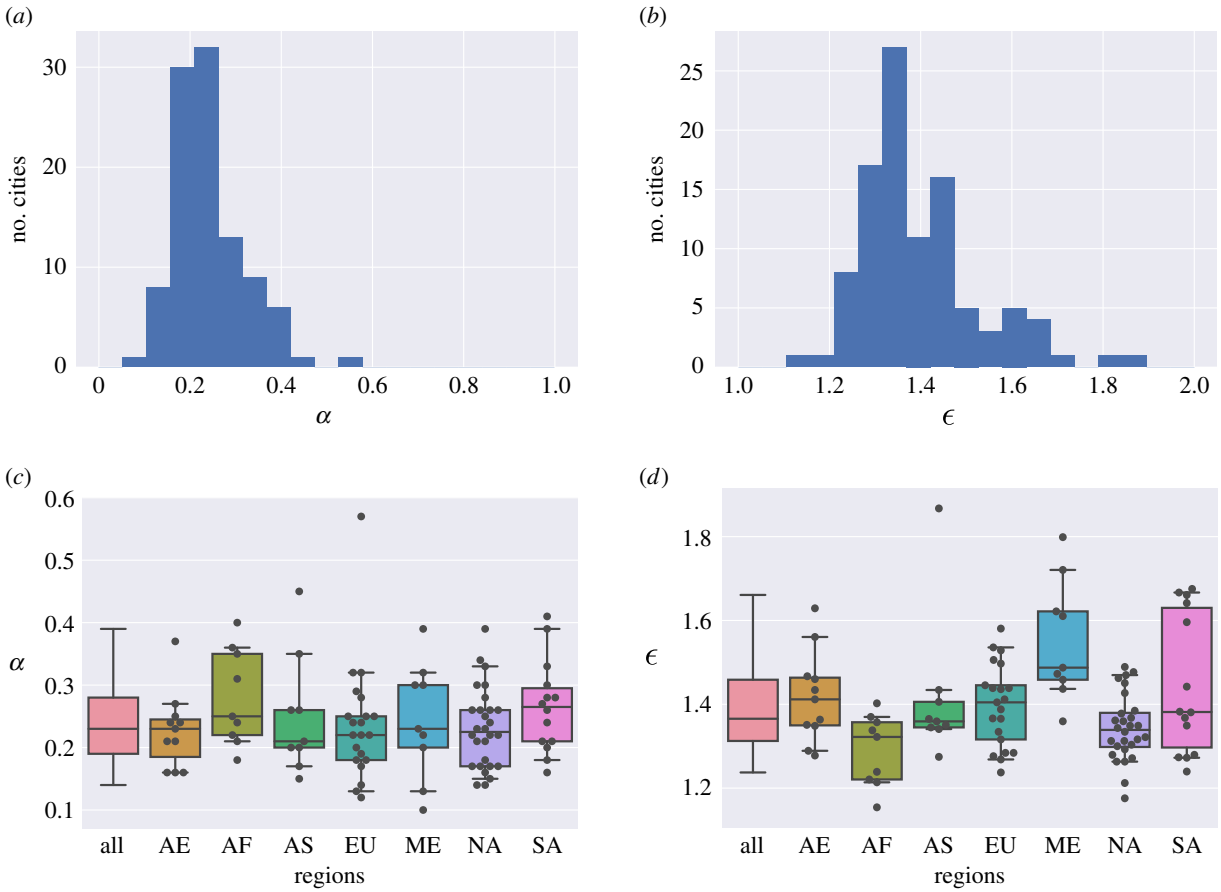


**Figure 3.** Distribution of trade-offs and distances to the Pareto front for all cities. (*a*,*b*) Histograms of $\alpha$ and $\epsilon$ show a limited range over the broad range of cities studied. (*c*,*d*) Distribution of $\alpha$ and $\epsilon$ broken down by geographical region (Asia East, Africa, Asia South, Europe, Middle East, North America, South America). More regional variation is seen in $\epsilon$ over $\alpha$. Whiskers are at 5th/95th percentile. (Online version in colour.)

graph-theoretic algorithm, most cities still performed better than baseline algorithms (Random, PrefAttach), which did not face such constraints.

We observed a range of $\epsilon$ values across the 101 cities, indicating that some cities were closer to the Pareto front than others (figure 2*b*). For example, Houston was relatively close to the Pareto front ($\epsilon = 1.26$), whereas Abbottabad was much further away ($\epsilon = 1.87$), and Melbourne was in between ($\epsilon = 1.40$). The topology of the travel paths of these cities was also quite diverse (figure 2*c*). For example, Fresno ($\epsilon = 1.21$) has many straight-lined paths indicative of a very grid-like topology, whereas Abbottabad ($\epsilon = 1.87$) has many jagged edges due to the mountainous region. Later, we study the effect of other city attributes (such as geography and land area) on $\epsilon$.

The overall range of $\epsilon$ values was limited (figure 3*b*); the mean $\bar{\epsilon} = 1.40$, with a small variance $\sigma_\epsilon^2 = 0.0175$. This indicates that most cities were within a relatively narrow band of optimality, despite the diversity of cities analysed.

## 3.7. Where near the Pareto front do cities tend to lie?

Next, we analysed where near the Pareto front the travel paths from each city lie. The smaller the value of $\alpha$, the more the travel paths look like the satellite tree, and the larger the $\alpha$, the more the paths resemble a spanning tree.

We observed $\alpha$ ranging from $\alpha = 0.57$ (Reykjavik), which favoured minimizing network length to $\alpha = 0.14$ (Ithaca), which minimized travel distance (figure 2*d*). The values of $\alpha$ were all less than 0.5, except for Reykjavik (mean $\bar{\alpha} = 0.243$, with variance $\sigma_\alpha^2 = 0.0062$; figure 3*a*). This again suggests that similar trade-offs between travel distance and network length are made by these diverse cities.

## 3.8. Do other city features correlate with Pareto optimality?

Here, we explore how $\epsilon$ (distance to the Pareto front) and $\alpha$ (trade-off) values for each city vary with three types of city measures: (i) city demographics, including metropolitan area population, age of the city and geographical region; (ii) traffic measures from Google Maps for each of our travel paths, including average number of manoeuvres (turns, merges, etc.), average speed with and without traffic, average travel time with and without traffic, and the traffic slowdown factor (the ratio of speed with traffic over speed without traffic); and (iii) additional traffic measures that are not specific to our travel paths but rather to the city as a whole. These measures are collected from the 2016 INRIX Global Traffic Scorecard [42]. The INRIX data were only available for 46 of the 101 cities and included peak hours spent in congestion (relevant for a rush-hour commuter), percentage of time spent in congestion (an overall congestion index using congestion rates weighted to account for the typical driver and a city's average journey times), and an overall ranking of cities (by peak hours spent in congestion, where a rank of 1 signifies the worst).

We found significant positive correlations between $\epsilon$ and the average number of manoeuvres and the travel time with and without traffic (table 1). This lends credence to our

**Table 1.** Pearson correlation coefficient ($r$) and $p$-value for $\alpha$ and $\epsilon$ versus city attributes. Significant correlations are shown in italics. Attributes that are significant after a Bonferroni correction ($n = 13$) are denoted with an asterisk.

| | $\alpha$ | | $\epsilon$ | |
|---|---|---|---|---|
| attribute | $r$ | $p$-value | $r$ | $p$-value |
| population | *− 0.216* | *0.0309* | 0.051 | 0.6162 |
| area | 0.040 | 0.6921 | 0.189 | 0.0611 |
| age | *− 0.212* | *0.0331* | 0.180 | 0.0712 |
| average number of manoeuvres | − 0.071 | 0.4850 | *0.381* | *<0.0001** |
| average speed | 0.119 | 0.2369 | − 0.116 | 0.2512 |
| average speed in traffic ($\sigma$) | 0.156 | 0.1183 | − 0.123 | 0.2212 |
| average time | 0.071 | 0.4834 | *0.485* | *<0.0001** |
| average time in traffic | 0.006 | 0.9517 | *0.457* | *<0.0001** |
| traffic slowdown factor | *0.260* | *0.0089* | − 0.047 | 0.6438 |
| INRIX hours spent in congestion | − 0.081 | 0.5914 | 0.143 | 0.3433 |
| INRIX congestion index | − 0.079 | 0.6041 | 0.188 | 0.2102 |
| INRIX all cities congestion rank | 0.007 | 0.9619 | *− 0.372* | *0.0109* |
| INRIX percentage of time in congestion | − 0.077 | 0.6119 | *0.451* | *0.0016** |

model, showing that cities that were further from the Pareto front yielded longer travel times and more manoeuvres per travel path. We also found significant, albeit slightly weaker, correlations between $\epsilon$ and the INRIX congestion rank and per cent time in congestion, which similarly suggests that cities further away from the Pareto front are more susceptible to traffic jams.

For $\alpha$, there was a weak correlation with population and age (table 1), suggesting that smaller and younger cities are more satellite in nature. Furthermore, the weak correlation of $\alpha$ with the traffic slowdown factor suggests that the more satellite-tree-like a city is, the greater effect traffic congestion has. Other studies have found relationships with travel miles and gross domestic product [43].

Next, we studied how $\alpha$ and $\epsilon$ vary according to regional differences (figure 3*c*,*d*). For each region, we performed a Kolmogorov–Smirnov test between the cities in that region and the cities in all other regions, to test if the region had a significantly different distribution of $\alpha$ or $\epsilon$ values compared to the rest of the world. For $\epsilon$, we found that the Middle East had significantly larger values of $\epsilon$ (i.e. was more sub-optimal) compared to the rest of the world ($p = 0.002$), whereas North America and Africa had slightly lower values of $\epsilon$ ($p = 0.051$ and $p = 0.063$, respectively). For $\alpha$, we find no significant differences between regions.

Thus, terrain appears to influence $\epsilon$ more so than $\alpha$. The eight cities with the highest values of $\epsilon$, specifically, Abbottabad ($\epsilon = 1.87$), Jerusalem ($\epsilon = 1.80$), Byblos ($\epsilon = 1.72$), Medellin ($\epsilon = 1.68$), Cusco ($\epsilon = 1.67$), Rio de Janeiro ($\epsilon = 1.66$), Caracas ($\epsilon = 1.64$) and Taipei ($\epsilon = 1.63$), are all in mountainous or hilly areas that require construction of winding roads (figure 2*c*). On the other hand, a number of the lowest $\epsilon$ cities are flat, namely Juba ($\epsilon = 1.15$), Fresno ($\epsilon = 1.21$), Harare ($\epsilon = 1.21$) and Kampala ($\epsilon = 1.22$). This was in contrast to $\alpha$, where three of the 10 highest and three of the 10 lowest $\alpha$ cities were mountainous: Abbottabad ($\alpha = 0.35$), Rio de Janeiro ($\alpha = 0.39$) and Cusco ($\alpha = 0.41$); Byblos ($\alpha = 0.1$), Barcelona ($\alpha = 0.13$) and Ithaca ($\alpha = 0.14$).

The impact of terrain on Pareto trade-offs is further supported by a positive correlation between $\epsilon$ and $\alpha$, ($r = 0.248$, $p = 0.0131$) indicating that cities that lie far from the Pareto front also require more indirect travel. Obstacles that raise the cost of construction and block direct paths, e.g. mountainous regions, may cause this.

We also assessed how proximity to a large body of water influenced transport efficiency in a city. Specifically, for each city, we manually inspected its terrain and classified it as being bordered by water (including being adjacent to oceans, or near bays and major rivers), or otherwise. We found no significant difference in the distributions of $\epsilon$ nor $\alpha$ values for cities near water versus otherwise (Kolmogorov–Smirnoff test, $p = 0.510$, 0.738 for $\epsilon$ and $\alpha$, respectively). In many cases, this was because there was no need for the road network to traverse the obstacle, e.g. the city was coastal. Examples include Osaka ($\epsilon = 1.34$) and Vancouver ($\epsilon = 1.35$). Otherwise, bridges enabled efficient connectivity over bays and rivers, such as in San Francisco and London (both $\epsilon = 1.34$), and Portland, Oregon ($\epsilon = 1.37$).

Overall, these results suggest that the closer a city lies to the Pareto front, the shorter the travel times and the better it deals with traffic congestion. Geography also imposes some constraints, especially those cities in mountainous regions. Interestingly, there was little effect of these city features on $\alpha$; the tight distribution of $\alpha$ (figure 3*a*) suggests that the trade-off between total length and travel distance used may be similar globally.

### 3.9. A higher-order Pareto front to further bound travel path complexity

Many cities lie near the Pareto front; however, there were some exceptions to this rule, indicating that other optimization factors or constraints also influence travel path structure. Ideally, there would be a simple way to incorporate additional objectives (e.g. travel time, traffic congestion, number of manoeuvres) into a joint optimization framework

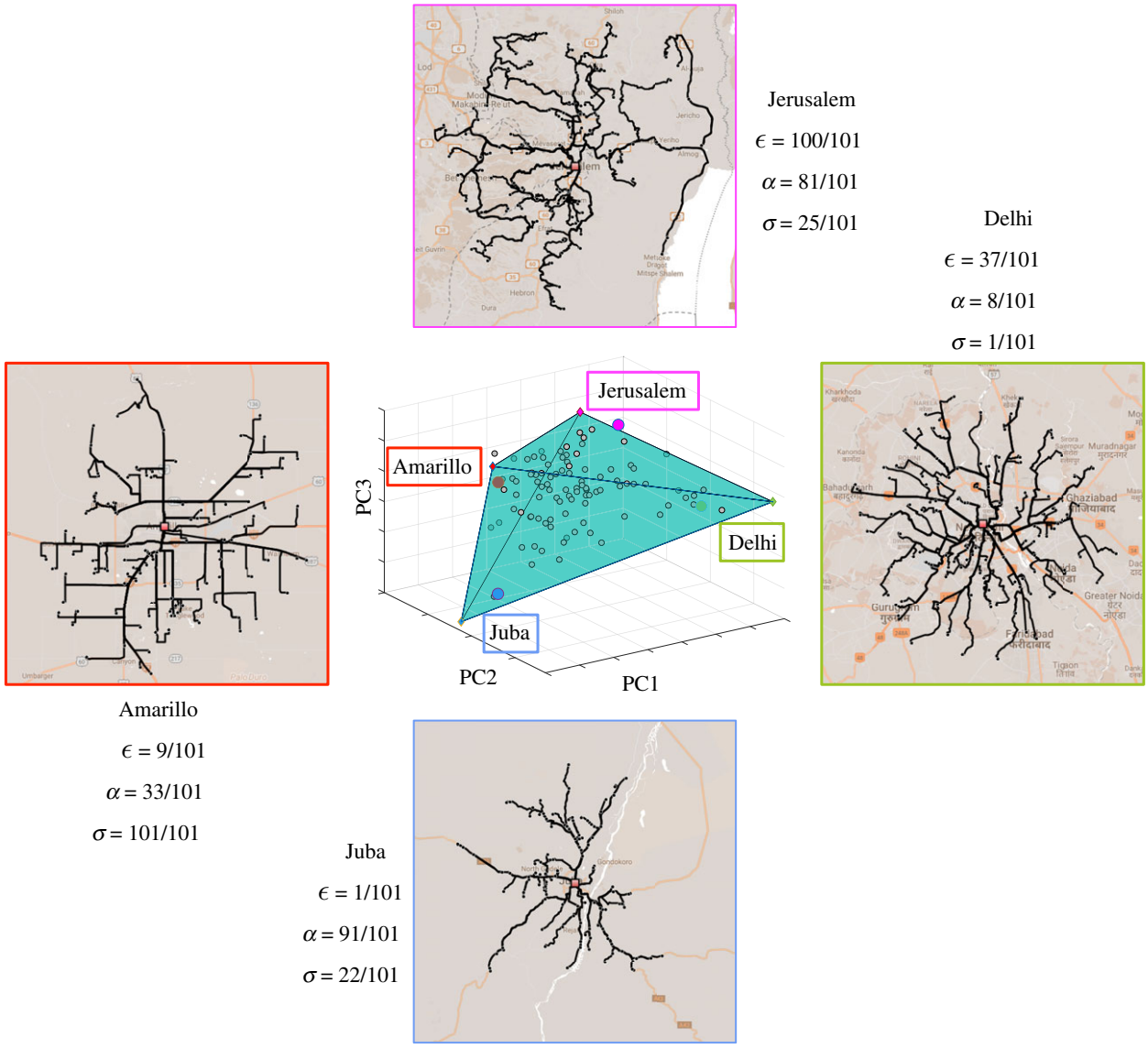


**Figure 4.** Archetype analysis of five-dimensional travel path space. The four cities closest to the three-dimensional simplex archetypes (corners) are shown. These cities show extreme behaviour in $\epsilon$, $\alpha$ and $\sigma$ (representing average speed in traffic). The rankings of each city over all 101 cities are shown; a high $\epsilon$ means the travel paths for the city lie far from the Pareto front; a high $\alpha$ indicates optimization of construction costs over travel distance; and a high $\sigma$ signifies high travel speed. (Map data: Google, Mapa GISrael, ORION-ME.) (Online version in colour.)

amenable to Pareto analysis. However, this would create several more variables to parameterize, including weighing factors among objectives. We are not aware of a theoretical model that describes these trade-offs for studying travel paths.

Instead, we leverage recent advances in Pareto optimality that seek to find 'archetypes' by analysing the dimensionality of traits of travel paths. Specifically, we used the `PartTI` package [44] to analyse five traits of the 101 cities: travel distance, network length, average travel speed, traffic slowdown factor (speed decrease due to traffic congestion), and number of manoeuvres. The latter three traits were derived from our Google Maps dataset (Methods). Overall, this generated a matrix with 101 rows (cities) and five columns corresponding to the five traits for each city.

`PartTI` performed a principal component analysis (PCA) on the $z$-score normalized matrix, and then attempted to enclose the 101 points in the reduced-dimensional space with a minimum-volume simplex (an $n$-dimensional triangle). We found that the cities in this five-dimensional space were well bounded within a tetrahedral simplex in a three-dimensional principal component subspace. This simplex had an explained variance of 73.5% and contained 80 of 101 cities (figure 4). This three-dimensional subspace is spanned by four corner points, or 'archetypes'. These archetypes represent extremal variations in travel path structures, whose traits can reveal how the five different traits may be weighed differently. They can also be viewed as a type of 'dictionary' that encodes the diversity of travel path structures across cities.

The four cities closest to the four archetypes were Amarillo, Jerusalem, Juba and Delhi (figure 4). These cities showed different trade-offs with respect to their rankings of $\epsilon$, $\alpha$ and $\sigma$, a new variable representing the average speed in the presence of traffic (lower is worse). Amarillo had the fastest travel speeds (highest $\sigma$) and had the ninth lowest $\epsilon$ (lying relatively close to the Pareto front). Jerusalem, on the other hand, was far from the Pareto front (second-worst $\epsilon$) and had relatively slow traffic (low $\sigma$), but had a high value of $\alpha$, meaning it was spanning-tree-like. Similarly, Delhi exhibited the absolute slowest traffic, but in contrast to Jerusalem, had the eighth lowest value of $\alpha$, meaning it was satellite-like. Finally, Juba

had the lowest value of $\epsilon$ (very close to the Pareto front) with the 10th highest value of $\alpha$ (spanning-tree-like), but showed low speeds in traffic. We also used feature enrichment analysis from the package, which similarly found that $\epsilon$ and $\alpha$ were properties statistically enriched near the archetypes (electronic supplementary material, `ParTI` Feature Enrichment Analysis, table S1).

Overall, our theoretical model found that travel paths within many cities were nearly Pareto optimal with respect to a trade-off between road length and travel distance; when adding three additional time-related variables, the Pareto space only increased by roughly one dimension. Therefore, our archetype analysis showed that time may be described as a single factor in the network.

## 4. Discussion

We showed that travel paths in road networks provide transport in a nearly Pareto optimal manner, with topologies that trade-off network length versus travel distance. When also including time-related measures, cities were bounded by only four archetypical topologies, suggesting that the design space of travel paths is encapsulated by a few canonical structures. The closer a city lies to the Pareto front the shorter its travel times and less is the impact of traffic congestion. Finally, despite wide variation in city features, we found a very tight distribution of $\alpha$ values, suggesting that the balance between objectives across these cities was very similar, and perhaps, universal. These measures may give light to the objectives and cost functions that drive the formation and evolution of travel paths in road networks.

We analysed a set of 101 cities, selected to represent a broad range of population sizes, land areas and geographies, to test the generality of this trade-off principle. The cities selected varied in population by over four orders of magnitude, by land area by over three orders of magnitude, and by age by over three orders of magnitude. While the analysis of additional cities is possible via Google Maps, these cities appeared generally representative of the diversity of land structures in the world. We studied the effects of additional features, such as population size and geography, on the Pareto optimality of cities (table 1). Travel path structure, however, may also be effected by other features, including gross domestic product [43], culture or dominant mode of transportation.

Our study was not meant to analyse all objectives of a city-scale transport system. We focused on one important aspect of city travel, which was in part motivated by similar challenges faced by two biological transport systems, where there is a single 'city centre' (analogous to a neuron's soma or a plant's base) through which transport is organized. However, our general framework could be extended to study additional objectives, for example, those where users seek to travel to multiple locations. In the extreme case, where users desire fast transport from any location in the city to any other, the satellite structure would be replaced by a clique structure, which minimizes the distance between any pair of nodes in a network.

There are two reasons why exact Pareto optimality may be difficult to achieve by travel paths in city road networks. First, road growth is typically 'online', where some set of roads are initially built, and then, based on feedback and demand, subsequent roads are built. This hampers optimality because design decisions made earlier in time strongly constrain those that are made subsequently. Our Pareto front generation algorithm, on the other hand, assumed that all the information about which points to connect was provided *a priori*. Thus, some difference in performance of 'online' versus 'offline' network design should be expected, and future work should attempt to quantify this gap. Second, road networks typically do not 'prune' the past; i.e. road networks rarely exhibit the abandonment of large stretches of road. This can also affect optimality because past decisions may no longer be as beneficial under current demands. Despite these limitations, city networks have managed to achieve a level of Pareto optimality that is significantly higher than baseline networks.

Finally, our work was motivated by prior analyses of Pareto-optimal transport in two biological structures, an observation we sought to test here for a human engineered system. The extent of Pareto optimality remains debated in biology. For example, Barve & Wagner [45] show that metabolic traits may have non-adaptive origins, and Valverde *et al.* [46] suggest that ecological networks have traits that represent evolutionary spandrels. Thus, we do not expect that all biological networks make Pareto-optimal trade-offs, and understanding the evolutionary trajectories that gave rise to these structures remains important.

However, at least two biological transport networks demonstrate Pareto-optimal trade-offs. First, plant shoot (above-ground) architectures can be viewed as transport networks, where the leaves are analogous to the locations $\mathcal{P}$ in the city, and the base of the plant is considered downtown (root, $r$). For plants, travel distance corresponds to a measure of how efficiently nutrients (e.g. sugars) can be transported along the branching architectures; network length measures how much resources are required to build the architecture. Conn *et al.* [26] showed that plant architectures for several species are Pareto optimal under the same cost-performance trade-off considered here. Second, neural branching arbors (dendrites and axons) can also be viewed as transport networks used to transmit information from one neuron to another. Here, the locations $\mathcal{P}$ correspond to the locations of synapses, and the root corresponds to the cell soma. Travel distance corresponds to a measure of conduction delay, which seeks to minimize the time required to transmit a signal from one neuron to another; network length is a measure of arbor wiring length, which is a commodity in space-constrained brains [27,28]. On a higher level, it has been shown that minimizing feedback latency, including transport times, is critical for the performance of biological control systems such as bipedal balance and locomotion [47,48]. Finally, there may also be other biological transport networks constrained by these principles, such as vascular networks that deliver oxygen throughout the body [49–52], and other nutrient supply networks [53,54]. Thus, similar network design principles shape the design of some biological and engineered structures.

## 5. Methods

### 5.1. Travel path data

We obtained travel path data from Google Maps via the Directions API [25]. Routing data for each travel path were requested for Wednesday, 13 December 2017 at 12.00 noon

local time, run on 5 December 2017, about one week in advance. This allowed the routes to consider a moderate level of traffic, while avoiding congestion found during rush hour. Additionally, the future date meant one-time events, such as accidents, were not considered. The destination point, downtown, was the default destination for the city returned by Google Maps. If a default was undefined (applicable to only approx. 10 cities), downtown was manually chosen.

We attempted to use the same set of 120 origin points for every city, with respect to distance and azimuth, however, certain paths returned by Google Maps were unable to be routed, or clearly unrepresentative of typical road travel patterns. This was because the origin point was placed in an inaccessible or uninhabited location, such as an island, body of water, or an area without roads. In some of these cases, Google Maps attempted to snap the origin point to ferries or to roads many kilometres away. Thus, points were rejected if the snapping distance was greater than $\pi/120 \approx 2.6\%$ of the distance from the point to downtown. Additionally, if a ferry was required or the path had a length of over 10 times the straight-line distance, the point was rejected as well. We replaced rejected points with the next points from the same random sequence. Finally, to remove outliers, the five longest paths were removed, leaving 115 total paths for each city.

The travel distance for each path was provided by the Google Maps API. To determine the total length of the utilized road network, all paths were merged. The API returns each path as a series of latitude/longitude points, which are not identical across multiple paths that share the same road. Therefore, we wrote an overlap detection algorithm that considered points that were closer than 100 m to be sharing the same road, so the duplicate path section between such points was removed. The length of the remaining sections were then summed to determine the network length.

The 120 origin points represented, on average, 1 point every 1.3 km$^2$, which is smaller than the area of most neighbourhoods. Thus, higher sampling density would likely select points within similar neighbourhoods, which would have similar travel paths. We also considered origin points located in a circle of radius 5, 15 and 30 km from downtown. We found that the $\alpha$ and $\epsilon$ values for these three datasets were well-correlated with the random set, with Pearson correlations $r_\alpha = [0.46, 0.72, 0.61]$ and $r_\epsilon = [0.58, 0.91, 0.90]$ for radii of [5, 15, 30] km respectively, suggesting that 120 origin points was adequate.

## 5.2. Greedy algorithm to generate a near-optimal Pareto front

The algorithm used to generate the Pareto front (i.e. to minimize equation (3.4) for a given value of $\alpha$) was described in Conn *et al.* [26], and a similar algorithm was used by Gastner *et al.* [17]. The algorithm is initialized with just the root node in the tree. In each step of the greedy algorithm, an edge is added that connects a node outside the tree to a node within the tree that minimizes equation (3.4). Steiner nodes may also be added along each edge to offer more potential edges to consider in each step, at the expense of longer running time. While this method is clearly not optimal—as minimizing equation (3.4) is NP-hard—Conn *et al.* [26] provide evidence that this method generates very close to optimal trees and outperforms prior heuristics for this problem.

Our greedy algorithm does not generate the Pareto-optimal front, as finding this front is an NP-hard problem [26]. However, this algorithm has been shown effective for approximating the Pareto front, and performs comparably to the optimal Steiner tree for $\alpha = 1$. Other heuristics, for example, based on genetic algorithms [55] and other graph-theoretic optimizations [56], were found to be too slow and generally worst-performing, respectively, compared to the greedy algorithm [29]. Thus, while our greedy algorithm is effective in practice, finding near-optimal Pareto fronts for large point sets and all values of $\alpha$ remains an open problem.

## 5.3. Archetype analysis and traffic data

Traffic data, used in both the correlation and archetype analysis, was obtained from Google Maps. Estimated trip times, without the impact of traffic, was returned with each travel path. Where Google Maps had traffic data, the trip time including the impact of traffic was obtained, using Google Maps' congestion model at the aforementioned 12.00 noon, local time.

Average speed was determined by the sum of all trip lengths in a city divided by the sum of the trip times. The traffic slowdown factor was the ratio of the sum of trip times without traffic to that with traffic. Thus, 1 indicates no traffic, and 0.5 indicates speed halved on average due to traffic. Finally, the average number of manoeuvres per trip, as returned by Google Maps, counted both turns, roundabout use, road forks, merges and exits on ramps. Straight travel through highway interchanges were counted as a manoeuvre, but not straight travel through surface street intersections [25].

For archetype analysis with the `ParTI` package [44], each variable was first $z$-score normalized. The package calculated the simplex using the `PCHA` algorithm, and the number of archetypes was determined using the elbow method. The cities closest to the archetypes were found in regards to the $\ell^2$-norm of the principal components.

Data accessibility. The data produced by the algorithms, demographic information used, and downtown coordinates are provided as a comma-separated value (CSV) file available as electronic supplementary material. The electronic supplementary material also lists the same data in tabular format, as well as plots the Pareto trade-off curves for all 101 cities. Source code is available at https://bitbucket.org/navlakha/city_pareto.

Author contributions. J.Y.S. and S.N. conceived the study, gathered and analysed the data, and wrote the manuscript.

Competing interests. We declare we have no competing interests.

Funding. S.N. was supported by the Pew Charitable Trusts, the National Science Foundation under award CAREER DBI-1846554, and the NIDCD of the National Institutes of Health under award number 1R01DC017695.

# References


1. Jay S, Illic D, Plückebaum T, Zoz K. 2012 Bottom-up cost model for the fixed access network in Spain. Technical report. Rhündorfer Str. 68, 53604 Bad Honnef, WIK-Consult GmbH, Germany.
2. Chen J, Wosinska L, Machuca CM, Jaeger M. 2010 Cost vs. reliability performance study of fiber access network architectures. *IEEE Commun. Mag.* **48**, 56–65. (doi:10.1109/MCOM.2010.5402664)
3. Swamee PK, Sharma AK. 2008 *Design of water supply pipe networks*. New York, NY: Wiley.
4. Pagani GA, Aiello M. 2013 The power grid as a complex network: a survey. *Physica A* **392**, 2688–2700. (doi:10.1016/j.physa.2013.01.023)
5. Akkaya K, Younis M. 2005 A survey on routing protocols for wireless sensor networks. *Ad Hoc Netw.* **3**, 325–349. (doi:10.1016/j.adhoc.2003.09.010)
6. Magnanti TL, Wong RT. 1984 Network design and transportation planning: models and algorithms. *Transp. Sci.* **18**, 1–55. (doi:10.1287/trsc.18.1.1)
7. Xie F, Levinson D. 2007 Measuring the structure of road networks. *Geogr. Anal.* **39**, 336–356. (doi:10.1111/gean.2007.39.issue-3)

8. Kalapala V, Sanwalani V, Clauset A, Moore C. 2006 Scale invariance in road networks. *Phys. Rev. E* **73**, 026130. (doi:10.1103/PhysRevE.73.026130)
9. Zhang H, Li Z. 2012 Fractality and self-similarity in the structure of road networks. *Ann. Assoc. Am. Geogr.* **102**, 350–365. (doi:10.1080/00045608.2011.620505)
10. Snelder M, Wagelmans AP, Schrijver JM, van Zuylen HJ, Immers LH. 2005 Optimal redesign of the Dutch road network. Technical report no. EI 2005-55. Delft, Econometric Institute, TNO, The Netherlands.
11. Beaven PJ, Lawrance CJ. 1982 Terrain evaluation for highway planning and design. *Transp. Res. Rec.* **892**, 36–46.
12. Nilsson J-E. 1991 Investment decisions in a public bureaucracy: a case study of Swedish road planning practices. *J. Transp. Econ. Policy* **25**, 163–175.
13. Laurance WF *et al.* 2014 A global strategy for road building. *Nature* **513**, 229–232. (doi:10.1038/nature13717)
14. Cotilla-Sanchez E, Hines PDH, Barrows C, Blumsack S. 2012 Comparing the topological and electrical structure of the North American electric power infrastructure. *IEEE Syst. J.* **6**, 616–626. (doi:10.1109/JSYST.2012.2183033)
15. Dunn S, Wilkinson S, Ford A. 2016 Spatial structure and evolution of infrastructure networks. *Sustain. Cities Soc.* **27**, 23–31. (doi:10.1016/j.scs.2016.08.011)
16. Lee M, Barbosa H, Youn H, Holme P, Ghoshal G. 2017 Morphology of travel routes and the organization of cities. *Nat. Commun.* **8**, 2229. (doi:10.1038/s41467-017-02374-7)
17. Gastner MT, Newman MEJ. 2006 Shape and efficiency in spatial distribution networks. *J. Stat. Mech: Theory Exp.* **2006**, P01015. (doi:10.1088/1742-5468/2006/01/P01015)
18. Wang P, Liu L, Li X, Li G, González MC. 2014 Empirical study of long-range connections in a road network offers new ingredient for navigation optimization models. *New J. Phys.* **16**, 013012. (doi:10.1088/1367-2630/16/1/013012)
19. Yuan J, Zheng Y, Zhang C, Xie W, Xie X, Sun G, Huang Y. 2010 T-drive: driving directions based on taxi trajectories. In *Proc. of the 18th SIGSPATIAL Int. Conf. on Advances in Geographic Information Systems. GIS '10. San Jose, CA*, pp. 99–108. New York, NY: ACM.
20. Yang H, Yagar S, Iida Y. 1994 Traffic assignment in a congested discrete/continuous transportation system. *Transp. Res. B: Methodol.* **28**, 161–174. (doi:10.1016/0191-2615(94)90023-X)
21. Yan X, Radwan E. 2007 Effect of restricted sight distances on driver behaviors during unprotected left-turn phase at signalized intersections. *Transp. Res. Part F: Traffic Psychol. Behav.* **10**, 330–344. (doi:10.1016/j.trf.2007.01.001)
22. Mainali MK, Mabu S, Yu S, Eto S, Hirasawa K. 2010 Dynamic optimal route search algorithm for car navigation systems with preferences by dynamic programming. *IEEJ Trans. Electr. Electron. Eng.* **6**, 14–22. (doi:10.1002/tee.v6.1)
23. Linden S. 1986 Practical considerations in optimal flight management computations. *J. Guid. Control Dyn.* **9**, 427–432. (doi:10.2514/3.20128)
24. Boyce D, Xiong Q. 2004 User-optimal and system-optimal route choices for a large road network. *Rev. Netw. Econ.* **3**, 371–380. (doi:10.2202/1446-9022.1058)
25. Google. Directions API. Developer guide. https://developers.google.com/maps/documentation/directions/intro.
26. Conn A, Pedmale UV, Chory J, Navlakha S. 2017 High-resolution laser scanning reveals plant architectures that reflect universal network design principles. *Cell Syst.* **5**, 53–62. (doi:10.1016/j.cels.2017.06.017)
27. Budd JM, Kováacs K, Ferecskó AS, Buzás P, Eysel UT, Kisvárday ZF. 2010 Neocortical axon arbors trade-off material and conduction delay conservation. *PLoS Comput. Biol.* **6**, e1000711. (doi:10.1371/journal.pcbi.1000711)
28. Cuntz H, Forstner F, Borst A, Häusser M. 2010 One rule to grow them all: a general theory of neuronal branching and its practical application. *PLoS Comput. Biol.* **6**, e1000877. (doi:10.1371/journal.pcbi.1000877)
29. Chandrasekhar A, Navlakha S. 2019 Neural arbors are Pareto optimal. *Proc. R. Soc. B* **286**, 20182727. (doi:10.1098/rspb.2018.2727)
30. Seoane LF, Solé R. 2015 Phase transitions in Pareto optimal complex networks. *Phys. Rev. E* **92**, 032807. (doi:10.1103/PhysRevE.92.032807)
31. Seoane LF, Solé R. 2016 Multiobjective optimization and phase transitions. In *Proc. of ECCS 2014*. (eds S Battiston, F De Pellegrini, G Caldarelli, E Merelli), pp. 259–270. Cham, Switzerland: Springer International Publishing.
32. Avena-Koenigsberger A, Goñi J, Solé R, Sporns O. 2015 Network morphospace. *J. R. Soc. Interface* **12**, 20140881. (doi:10.1098/rsif.2014.0881)
33. Moses M, Bezerra G, Edwards B, Brown J, Forrest S. 2016 Energy and time determine scaling in biological and computer designs. *Phil. Trans. R. Soc. B* **371**, 20150446. (doi:10.1098/rstb.2015.0446)
34. Pardalos PM, Migdalas A, Pitsoulis L (eds). 2008 *Pareto optimality, game theory and equilibria. Springer optimization and its applications*, vol. 17. New York, NY: Springer.
35. Diamond PA, Mirrlees JA. 1971 Optimal taxation and public production I: production efficiency. *Am. Econ. Rev.* **61**, 8–27.
36. Samuelson PA. 1954 The pure theory of public expenditure. *Rev. Econ. Stat.* **36**, 387–389. (doi:10.2307/1925895)
37. Shoval O, Sheftel H, Shinar G, Hart Y, Ramote O, Mayo A, Dekel E, Kavanagh K, Alon U. 2012 Evolutionary trade-offs, Pareto optimality, and the geometry of phenotype space. *Science* **336**, 1157–1160. (doi:10.1126/science.1217405)
38. Tullock G. 1971 Biological externalities. *J. Theor. Biol.* **33**, 565–576. (doi:10.1016/0022-5193(71)90097-X)
39. Handl J, Kell DB, Knowles J. 2007 Multiobjective optimization in bioinformatics and computational biology. *IEEE/ACM Trans. Comput. Biol. Bioinf.* **4**, 279–292. (doi:10.1109/TCBB.2007.070203)
40. Heinrich R, Schuster S. 1996 *The regulation of cellular systems*. London, UK: Chapman & Hall.
41. Barabási A-L, Albert R. 1999 Emergence of scaling in random networks. *Science* **286**, 509–512. (doi:10.1126/science.286.5439.509)
42. Cookson G, Pishue B. 2017 INRIX global traffic scorecard. Technical report no. 10210 NE Points Drive, Suite 400, Kirkland, WA 98033. INRIX Research, United States.
43. Bettencourt LMA. 2013 The origins of scaling in cities. *Science* **340**, 1438–1441. (doi:10.1126/science.1235823)
44. Hart Y, Sheftel H, Hausser J, Szekely P, Ben-Moshe NB, Korem Y, Tendler A, Mayo AE, Alon U. 2015 Inferring biological tasks using Pareto analysis of high-dimensional data. *Nat. Methods* **12**, 233–235. (doi:10.1038/nmeth.3254)
45. Barve A, Wagner A. 2013 A latent capacity for evolutionary innovation through exaptation in metabolic systems. *Nature* **500**, 203. (doi:10.1038/nature12301)
46. Valverde S, Piñero J, Corominas-Murtra B, Montoya J, Joppa L, Solé R. 2018 The architecture of mutualistic networks as an evolutionary spandrel. *Nat. Ecol. Evol.* **2**, 94–99. (doi:10.1038/s41559-017-0383-4)
47. Milton J, Cabrera JL, Ohira T, Tajima S, Tonosaki Y, Eurich CW, Campbell SA. 2009 The time-delayed inverted pendulum: implications for human balance control. *Chaos: an Interdiscipl. J. Nonlinear Sci.* **19**, 026110. (doi:10.1063/1.3141429)
48. Doyle JC, Csete M. 2011 Architecture, constraints, and behavior. *Proc. Natl Acad. Sci. USA* **108**, 15 624–15 630. (doi:10.1073/pnas.1103557108)
49. Newberry MG, Ennis DB, Savage VM. 2015 Testing foundations of biological scaling theory using automated measurements of vascular networks. *PLoS Comput. Biol.* **11**, e1004455. (doi:10.1371/journal.pcbi.1004455)
50. Tekin E, Hunt D, Newberry MG, Savage VM. 2016 Do vascular networks branch optimally or randomly across spatial scales? *PLoS Comput. Biol.* **12**, e1005223. (doi:10.1371/journal.pcbi.1005223)
51. Murray CD. 1926 The physiological principle of minimum work: I. The vascular system and the cost of blood volume. *Proc. Natl Acad. Sci. USA* **12**, 207–214. (doi:10.1073/pnas.12.3.207)
52. Gafiychuk V, Lubashevsky I. 2001 On the principles of the vascular network branching. *J. Theor. Biol.* **212**, 1–9. (doi:10.1006/jtbi.2001.2277)
53. Dodds PS, Rothman DH, Weitz JS. 2001 Re-examination of the '3/4-law' of metabolism. *J. Theor. Biol.* **209**, 9–27. (doi:10.1006/jtbi.2000.2238)
54. West GB, Brown JH, Enquist BJ. 1997 A general model for the origin of allometric scaling laws in biology. *Science* **276**, 122–126. (doi:10.1126/science.276.5309.122)
55. Chen G, Chen S, Guo W, Chen H. 2007 The multi-criteria minimum spanning tree problem based genetic algorithm. *Inf. Sci.* **177**, 5050–5063. (doi:10.1016/j.ins.2007.06.005)
56. Khuller S, Raghavachari B, Young N. 1995 Approximating the minimum equivalent digraph. *SIAM J. Comput.* **24**, 859–872. (doi:10.1137/S0097539793256685)